Variational approach for uniformly frustrated 2D XY spin systems. I. Phase transitions in modulated arrays

D. Ariosa, A. Vallat, H. Beck

J. Phys. France **51** (1990) 1373-1386 1er JUILLET **1990,** PAGE 1373

Classification
Physics Abstracts
75.10H — 74.50

Variational approach for uniformly frustrated 2D *XY* spin systems. I. Phase transitions in modulated arrays

D. Ariosa, A. Vallat and H. Beck

Institut de physique, Université de Neuchâtel, Rue A.-L. Breguet 1, CH-2000 Neuchâtel, Switzerland

(*Reçu le 20 juillet 1989, révisé le 13 février 1990, accepté le 15 mars 1990*)

Résumé. — Pour clarifier la nature de la transition de phase du modèle *XY*-2D complètement frustré, nous étudions le cas d'un réseau avec des liaisons modulées, où la transition se dédouble en deux transitions distinctes. La méthode utilisée est une approximation harmonique autoconsistante (« SCHA ») qui nous fournit un système d'équations pour les couplages effectifs K_{ij} et les moyennes thermiques $\langle \theta_{ij} \rangle$ des différences angulaires entre plus proches voisins. Nous prédisons l'occurrence d'une transition de phase du type Ising, suivie à plus haute température d'une transition du type BKT. Dans le voisinage de la 1re transition, les équations SCHA ont été modifiées en accord avec les exposants critiques connus du modèle Ising-2D en évitant ainsi la divergence des fluctuations inhérente à la méthode. Dans le cas non modulé, les deux transitions sont confondues en une seule ayant un caractère mixte. La validité de « SCHA », reliée aux fluctuations de phase, est discutée. Nous comparons nos résultats à ceux obtenus avec une approche de type Champ Moyen sur un modèle à deux couches, à des simulations Monte-Carlo et à des résultats expérimentaux.

Abstract. — In order to clarify the nature of the phase transition taking place in the fully frustrated *XY* model, we examine the case of the array with modulated bonds, where one observes a splitting of this transition in two distinct ones. The method used is a Self Consistent Harmonic Approximation (SCHA) that provide us with a set of self consistent equations for effective couplings $K_{i,j}$ and for thermal averages of angular differences $\langle \theta_i - \theta_j \rangle$ between nearest neighbours. We predict the occurrence of an Ising like phase transition followed by one of the Berezinski-Kosterlitz-Thouless (BKT) type at higher temperatures. In the vicinity of the 1st transition, the SCHA equations were modified in accordance with the known critical exponents of the 2D-Ising model in order to avoid the divergence of phase fluctuations inherent to the method. For the unmodulated case both transitions merge in a single one of mixed character. The range of validity of the SCHA, related with the phase fluctuations, is discussed. The results are compared with those of the mean-field solution of a two-layer model, Monte-Carlo simulations and experimental data.

1. Introduction.

The 2D *XY* spin model describes the thermodynamic properties of planar arrays of proximity junctions. In recent years there has been a great deal of theoretical and experimental interest [1] in the properties of such arrays. When a transverse magnetic field is applied, the

system behaves as a frustrated XY model. In particular, a square lattice of such junctions in a transverse magnetic field with half of an elementary flux quantum per plaquette, corresponds to a fully frustrated XY model [2]. In this case, frustration introduces a discrete symmetry (related to the double degeneracy of the ground state) on top of the continuous symmetry (global rotation of the spins) already present in the unfrustrated case. These two distinct symmetries are related to two kinds of phase transitions : the Ising transition (driven by domain wall excitations) and the BKT one (driven by vortex excitations). Both experiments [3] and computer simulations [4, 7] show a single transition. However the occurrence of this single transition of mixed character is not yet well understood, since different approaches disagree about its nature.

The work by Berge *et al.* [5] was, to our knowledge, the first tentative to split these transitions by modifying the frustration through varying the stength of negative bonds of Villain's fully frustrated model [6]. They performed a Monte-Carlo simulation, finding the Ising transition preceding the BKT one in temperature. By looking at the cusp of the specific heat they conclude that for the transition in the non-modulated case the Ising character was dominant.

The same model was investigated recently by H. Eikmans *et al.* [7] ; this contribution contains two different and complementary approaches of the problem : a derivation of the Coulomb gas picture of the modulated system and a Monte-Carlo simulation. The first leads the authors to the conclusion that, in the modulated system, existence of dipoles of fixed length centered on the weak bonds can inhibit the formation of free fractional charges (responsible for the screening of the Coulomb interaction) associated with the growth of domains at the Ising transition. The helicity modulus (or inverse dielectric constant) will then contain an « energy like anomaly » at T_{IS} and will go to 0 at a higher temperature T_{BKT}. Both predictions were confirmed by the MC simulation. For further comparison with our variational approach, we want to focus on two particular results in reference [7] : the density of domain walls *vs.* temperature that supports the dipole picture, and the shape of helicity modulus that contains both the anomaly at T_{IS} and the jump at T_{BKT}.

The purpose of our paper is to investigate the frustrated and modulated (F-M) model, introduced by Berge [5], within the Self Consistent Harmonic Approximation (SCHA). In section 2 we recall the definition and the principal features of the model ; in section 3 we derive the set of equations for effective couplings K_{ij} and average angular differences $\langle \theta_i - \theta_j \rangle$. In section 4, we present an iterative method for solving the coupled equations of section 3. In section 5 we present the results for the helicity modulus, domain wall densities and the phase diagram for the double transition ; comparisons are made with other theoretical approaches [5, 7, 8] and experimental work [9]. We summarize our results and draw conclusions in section 6. Some precautions must be taken in evaluating thermal averages near the Ising critical point to avoid divergence of the fluctuations inherent to the SCHA. This point and other technical difficulties are discussed in the appendix.

2. The model.

Our starting point is the usual fully frustrated 2-D XY model. This model applies to an array of proximity junctions in a transverse magnetic field of flux $Ba^2 = \phi_0/2$ ($\phi_0 = \dfrac{hc}{2e}$ being the magnetic flux quantum and a the lattice constant). We thus consider the Hamiltonian :

$$H = -J \sum_{\langle i,j \rangle} \cos(\theta_i - \theta_j - A_{ij}) \qquad \text{with} \qquad A_{ij} = \frac{2\pi}{\phi_0} \int_i^j \mathbf{A} \cdot \mathbf{dl} \tag{2.1}$$

where $\mathbf{A}$ is the corresponding vector potential.

In the Landau gauge (i.e. $\mathbf{A} = (0, Bx, 0)$), the quantities A_{ij} are 0 for all horizontal bonds and $n_x \pi$ for vertical ones, located at horizontal distances $n_x a$ from the origin. Consequently Hamiltonian (2.1) can be written as follows :

$$H = - \sum_{\langle i,j \rangle} J_{ij} \cos (\theta_i - \theta_j) \tag{2.2}$$

with $J_{ij} = J$ for horizontal bonds and for bonds on every second vertical row, and $- J$ on the other half of vertical bonds.

The generalization introduced by Berge *et al.* [5], consists in multiplying the negative bonds by a factor α. A picture of the modulated array is shown in figure 1, where the dotted line encloses the unit cell of the array we shall consider in the next section, in accordance with the symmetries of the well known doubly degenerate ground state [2].

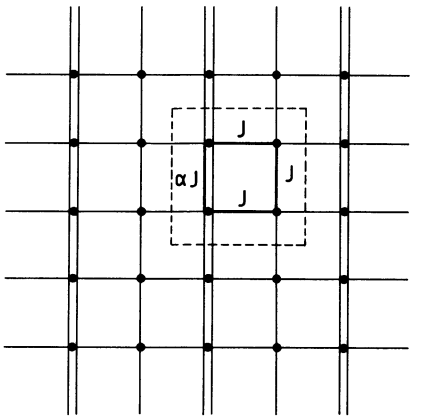

Fig. 1. — Modulated array. Double vertical lines stand for antiferromagnetic ($J < 0$) bonds. The dotted line encloses the unit cell of the ground state.

3. The variational equations.

We consider a trial Hamiltonian H_{TR}, quadratic in the deviations from thermal equilibrium of angular differences between nearest neighbours :

$$H_{\mathrm{TR}} = \frac{1}{2} \sum_{\langle i,j \rangle} K_{ij} (\phi_i - \phi_j)^2 \qquad \text{where} \qquad \phi_i = \theta_i - \langle \theta_i \rangle \ . \tag{3.1}$$

The variational free energy is given as usual by :

$$F = F_{\mathrm{TR}} + \langle H \rangle_{\mathrm{TR}} - \langle H_{\mathrm{TR}} \rangle_{\mathrm{TR}} \tag{3.2}$$

where the averages with the « TR » subscript have to be computed with the trial density matrix :

$$\rho_{\mathrm{TR}} = \mathrm{e}^{-\beta H_{\mathrm{TR}}} \quad \text{and} \quad Z_{\mathrm{TR}} = \mathrm{Tr}\ (\rho_{\mathrm{TR}}) \ . \tag{3.3}$$

Introducing (2.1) and (3.1) in expression (3.2) we obtain :

$$F = - \frac{1}{\beta} \ln Z_{\mathrm{TR}} - \sum_{\langle i,j \rangle} J_{ij} \cos (\langle \theta_i \rangle - \langle \theta_j \rangle) \, \mathrm{e}^{-\frac{1}{2} X_{ij}} - \sum_{\langle i,j \rangle} \frac{1}{2} K_{ij} X_{ij} \ . \tag{3.4}$$

with $\beta = \dfrac{1}{k_B T}$ and $X_{ij} = \langle (\phi_i - \phi_j)^2 \rangle_{TR}$.

The quantities X_{ij} are calculated, as usual, by the eigenvalues of the harmonic Hamiltonian H_{TR} (see appendix for some details). If we define the average current on the (i,j) bond by :

$$I_{ij} = J_{ij} \langle \sin(\theta_i - \theta_j) \rangle_{TR} = J_{ij} e^{-\frac{1}{2} X_{ij}} \sin(\langle \theta_i - \theta_j \rangle) \tag{3.5}$$

the minimization of F with respect to the parameters $\langle \theta_i \rangle$ yields the current conservation on every node of the array.

On the other hand, the minimization of F with respect to the parameters X_{ij} provides us with a set of self consistent equations for effective couplings :

$$K_{ij} = J_{ij} \cos(\langle \theta_i - \theta_j \rangle) e^{-\frac{1}{2} X_{ij}}. \tag{3.6}$$

Taking into account the symmetries of the system, we can define three non equivalent kinds of bonds : the horizontal bonds (subscript « h »), the unmodulated vertical bonds (subscript « v ») and the vertical modulated bonds (subscript « α »). If we define in addition, the bond variables :

$$\begin{aligned} \theta_h &= \langle \theta_1 - \theta_2 \rangle = \langle \theta_3 - \theta_4 \rangle \\ \theta_v &= \langle \theta_2 - \theta_3 \rangle \\ \theta_\alpha &= \langle \theta_4 - \theta_1 \rangle \end{aligned} \tag{3.7}$$

(where sites 1, 2, 3 and 4 are defined on a typical plaquette in Fig. 2), we can express the current conservation as follows :

$$\begin{aligned} \sin\theta_h e^{-\frac{1}{2}X_h} &= \sin\theta_v e^{-\frac{1}{2}X_v} \\ \sin\theta_h e^{-\frac{1}{2}X_h} &= \alpha \sin\theta_\alpha e^{-\frac{1}{2}X_\alpha}. \end{aligned} \tag{3.8}$$

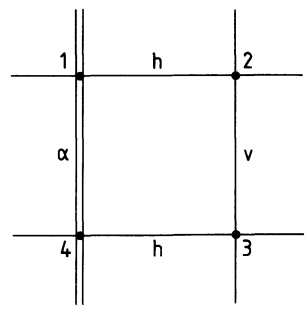

Fig. 2. — Labelling of the sites for a typical plaquette (see Eq. (3.7)).

With the additional condition

$$\theta_\alpha = 2\theta_h + \theta_v \tag{3.9}$$

(3.8) can be written in a more useful way :

$$\sin \theta_h = \sqrt{\frac{4\,\alpha^2 ab - (a-\alpha)^2}{4\,\alpha a(1+\alpha b)}}$$

$$\sin \theta_v = \sin \theta_h \, e^{-\frac{1}{2}(X_h - X_v)} \tag{3.10}$$

with $$a = e^{-\frac{1}{2}(X_v - X_\alpha)}$$

and $$b = e^{-\frac{1}{2}(X_v + X_\alpha - 2X_h)}$$

Using the same notations, the set of equations (3.6) reduces to three self consistent equations :

$$K_h = J \cos \theta_h \, e^{-\frac{1}{2}X_h}$$

$$K_v = J \cos \theta_v \, e^{-\frac{1}{2}X_v} \tag{3.11}$$

$$K_\alpha = -\alpha J \cos \theta_\alpha \, e^{-\frac{1}{2}X_\alpha}.$$

As a check, the ground state for a given alpha can be evaluated from (3.9) and (3.10) by making $X_h = 0$, $X_v = 0$ and $X_\alpha = 0$ $(T = 0)$:

$$\sin \theta_h = \sqrt{\frac{3\,\alpha - 1}{4\,\alpha}} \quad \text{and} \quad \theta_v = \theta_h = \frac{\theta_\alpha}{3}. \tag{3.12}$$

At $\alpha = 1$, we recover the well known result for the fully frustrated XY model. Notice that equations (3.12) admit non trivial solutions $(\theta_h \neq 0)$ only if $\alpha > \frac{1}{3}$.

In figure 3 we display the evolution of the ground state angular configuration when varying α.

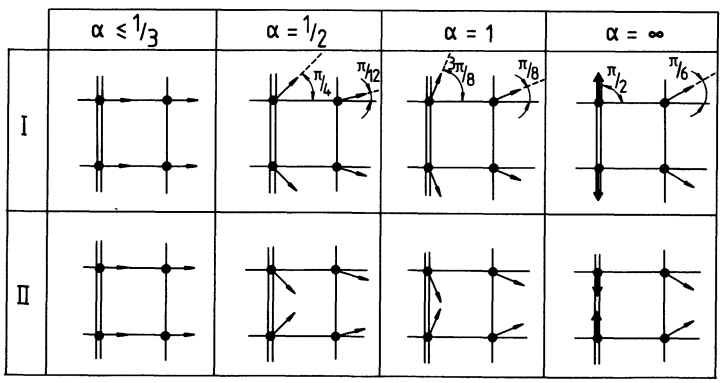

Fig. 3. — Evolution of the two degenerate ground state configurations when varying the modulation α.

4. Iterative solution of the SCHA equations.

The aim of our calculation is to get, for a given α, the evolution in temperature of both the effective couplings (K_h, K_v, K_α) and the equilibrium angular configuration $(\theta_h, \theta_v, \theta_\alpha)$.

The starting point is the ground state given by equations (3.9)-(3.11) at $T = 0$ (i.e. $X_h = X_v = X_\alpha = 0$). The iteration from a temperature T to a temperature $(T + \delta T)$ is performed in the following way :

a) we first change T by $(T + \delta T)$ in the density matrix of equation (3.3) ;

b) we then update the values of X_h, X_v and X_α using the updated density matrix and the last calculated values for K_h, K_v and K_α ;

c) we introduce the news X's in equations (3.10) in order to update the θ's.

d) the updated X's and θ's are then used to compute the K's through equations (3.11).

Steps b) to d) have to be repeated up to obtain stability of the results (in practice, for $\delta T = \frac{J}{k_B} 10^{-2}$, the procedure converges in less than four cycles).

All operations described above are straightforward except the thermal averaging using Eq. (3.3) in step b). This calculation is detailed in the appendix.

At this point, we should discuss the validity of SCHA on our specific system. Indeed, the original periodic potential in cos $(\theta_i - \theta_j)$ is replaced by an effective one in $(\phi_i - \phi_j)^2$; thus, for weak enough couplings K_{ij}, phase fluctuations (characterized by their quadratic mean $\sqrt{\langle (\phi_i - \phi_j)^2 \rangle_{TR}}$) can carry the average phase difference outside its definition interval $[-\pi, \pi]$. Furthermore, as pointed out by Fishman [10], even if the phase difference remains in its allowed interval, the approximation becomes doubtful for phase fluctuations of the order $\frac{\pi}{4}$. Fortunately in our case we can check, *a posteriori*, that average phase fluctuations are always well below $\frac{\pi}{2}$ (the value where the cosine curvature changes its sign) at equilibrium values of K_{ij} found self-consistently.

The eventual existence of another free energy minimum at lower values of K is not a problem for us since, starting from the known ground state, we follow the solution continuously in temperature. (This continuity argument must be reconsidered in the case of quantum fluctuations induced by charging effects [11].)

5. Results.

The procedure described in section 4 was used for different values of the modulation parameter α.

Figure 4 shows a typical result of our self consistent calculation ; the X and Y components of the anisotropic helicity modulus Γ (within our approximation $\Gamma_X = \frac{K_h}{J}$ and $\Gamma_Y = \frac{K_v + K_\alpha}{2J}$) are plotted *versus* the reduced temperature $t = \frac{e}{4} \cdot \frac{k_B T}{J}$ (we use the SCHA critical temperature of the unfrustrated and unmodulated system $Tc_0 = \frac{4}{e} \cdot \frac{J}{k_B}$ as our temperature unit [13]). The dotted line represents the Ising like order parameter $S = \sin(\theta_h)$, that goes rapidly to 0 at the Ising transition. Notice the singularity in the first derivative of Γ appearing at the same temperature where S goes to 0. Although this is obviously not apparent in the numerical curves, the cusp at T_{IS} corresponds to the logarithmic derivative singularity in the internal energy or the nearest neighbour correlation function of the 2D Ising model. This can be seen as follows : the renormalized force constants K_h, K_v and K_α depend, according to expressions (3.11) on the nearest neighbour fluctuations X_h, X_v and X_α which are given by expressions like (A7). In a mode decomposition the latter contain $\langle |\Phi_3(q)|^2 \rangle$, i.e. the fluctuations of the third mode which goes soft at T_{IS}. This mode

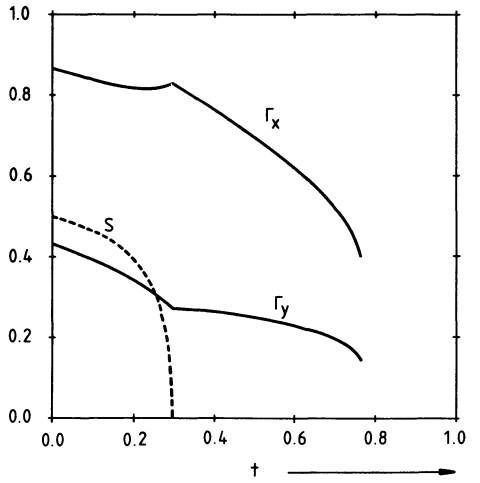

Fig. 4.

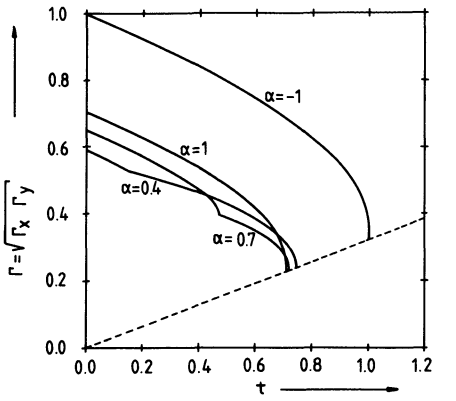

Fig. 5.

Fig. 4. — Two components of the helicity tensor $\Gamma_{\alpha\beta}$ (full line) and Ising like order parameter S (dotted line) *vs.* reduced temperature $t = \frac{e}{4} \cdot \frac{k_B T}{J}$ for $\alpha = 0.5$.

Fig. 5. — Helicity modulus Γ *vs.* reduced temperature t, for different values of the modulation parameter ($\alpha = -1$; 0.4 ; 0.7 and 1). (The dotted line is plotted to exhibit the universality of the jump).

belongs to the eigenvector $\mathbf{v}_3$ (see appendix) the form of which, at $q = 0$, is $(1, -1, +r_3, -r_3)$ with $r_3 = F + \sqrt{F^2 + 1} > 1$. This mode corresponds precisely to the pattern of the ground state of our system, in other words : rotations of the spins on the 4 sites of figure 3 by angles corresponding to the components of vector $\mathbf{v}_3$, starting from a ferromagnetic configuration, precisely generates the ground state pattern. One can thus interpret the field Φ_3 as representing, in the spirit of a « continuous spin » Φ^4-model, the Ising spin variable, and X_h, X_v and X_α corresponds to the Ising spin nearest neighbour fluctuations $\langle (S_i - S_{i+1})^2 \rangle = 2 - 2 \langle S_i \cdot S_{i+1} \rangle$. The correlation function $\langle S_i \cdot S_{i+1} \rangle$ have the same critical behaviour of $|T - T_c| \log (|T - T_c|)$ as the internal energy.

The same feature is observed for all values of α above $\frac{1}{3}$, i.e. an Ising like phase transition followed by one of BKT type at higher temperature.

The rapid drop of S reflects the fact that, above T_{IS}, the current conservation equations (3.10) admit only the trivial solution $\theta_h = \theta_v = \theta_\alpha = 0$. The jump of Γ at T_{BKT} reflects the fact that, for strong enough fluctuations, the self consistent equations (3.11) admit only the trivial solution $K_h = K_v = K_\alpha = 0$. (In fact, the free energy minimum disappears at this temperature, and constitutes the signature of the BKT transition in the harmonic approximation.)

The case $\alpha = 1$ (fully frustrated without modulation) is specially interesting to discuss : for $\alpha = 1$, $S = \frac{\sqrt{2}}{2}$ at $T = 0$ and all the K's are $\frac{\sqrt{2}}{2} J$. In increasing the temperature, the mean fluctuations on different bonds will evolve identically since they have the same starting strength. Thus, the quantities a and b of equations (3.10) will remain equal to unity and the average angular configuration will be constant up to the temperature above which the non trivial solution of equations (3.11) is no longer valid.

Bellow $\alpha = \frac{1}{3}$, $S = 0$ at all temperatures, thus the self consistent equations (3.11) evolve independently up to the jump at T_{BKT}. In figure 5, we show for comparison, the helicity modulus *versus* reduced temperature for four different systems : the simple unfrustrated array ($\alpha = -1$), the fully frustrated array without modulation ($\alpha = 1$) and two frustrated and modulated arrays ($\alpha = 0.4$ and 0.7). As in reference [7] we take into account the anisotropy by plotting the geometric mean $\Gamma = \sqrt{\Gamma_x \Gamma_y}$. At this point we want to stress that the present calculation is mainly aiming at studying the various aspects of the Ising transition. The B-K-T transition itself is probably no very well described by SCHA [14] ; although it does take thermal fluctuations into account, which renormalise the helicity modulus, as it is done by calculations based explicitly on the existence of vortices [15]. Nevertheless it is interesting to note the « universality » of the jump of Γ at the higher temperature transition.

The phase diagram (α, t_c) in figure 6 resumes the situation described above. Comparison of our results with the phase diagram of Berge *et al.* [5] and with the curves for helicity modulus of Eikmans *et al.* [7] (both obtained by Monte-Carlo simulation) are highly satisfactory. In addition our results agree with those obtained earlier by us in a mean field approach on a two-layer model [8]. Finally, recent measurements of the helicity modulus in square arrays of Josephson Junctions by Théron *et al.* [9] seem to show a weak singularity in agreement with our predictions.

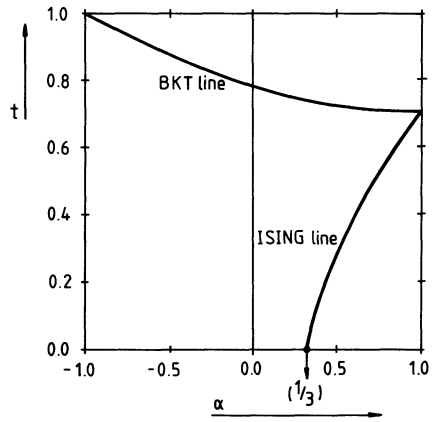

Fig. 6. — Phase diagram (α, t_c). Notice the absence of Ising transition below $\alpha = 1/3$.

The analysis of the helicity modulus only is, of course, not conclusive as to the nature of the transitions. In order to compare our results with the dipole picture of reference [7] we should evaluate, within our approach, the density of different types of domain walls at each temperature. To do it, we shall use a « zero current criterion » to detect domain boundaries in the system. This approximation, that clearly overestimates domain walls densities, is justified at low temperatures by the fact that minimal energy domain walls are centered on bonds through which there is zero current. In addition, within our variational approach we deal naturally with effective couplings and currents (see Eq. (3.5)) that are provided without additional numerical cost by the iterative procedure.

Let us write the probability for a certain bond (i, j) to be sitting on a domain wall as follows :

$$D_{ij}(t) = \langle \delta(\sin(\theta_i - \theta_j - A_{ij})) \rangle .$$

A truncated cumulant expansion, followed by a Gaussian integration gives :

$$\langle \delta (S) \rangle = \frac{e^{-\frac{1}{2}\frac{\langle S \rangle^2}{\langle S^2 \rangle_c}}}{\sqrt{2\pi \langle S^2 \rangle_c}} .$$

The quantities $\langle S \rangle^2$ and $\langle S^2 \rangle_c$, for $S = \sin(\theta_i - \theta_j - A_{ij})$, can be evaluated in the SCHA :

$$\langle S^2 \rangle_c = \frac{1}{2}\left[1 - \cos(2\langle \theta_i - \theta_j \rangle) e^{\frac{-X_{ij}}{2}}\right] - \langle S \rangle^2$$

and

$$\langle S \rangle^2 = \sin^2(\langle \theta_i - \theta_j \rangle) e^{-X_{ij}} . \tag{5.1}$$

Curves for D_{ij} *vs.* t on h, v and α-bonds are shown in figure 7 for three different values of the modulation parameter α. One can see from the plot that, excepting the isotropic case, the domain wall density on α-bonds is very small compared with those on unmodified vertical and horizontal bonds and it becomes important just close to the Ising point. The same qualitative behaviour was observed in reference [7], where the authors evaluate the densities of domain walls using nearest neighbour charge-charge correlation functions on the dual lattice.

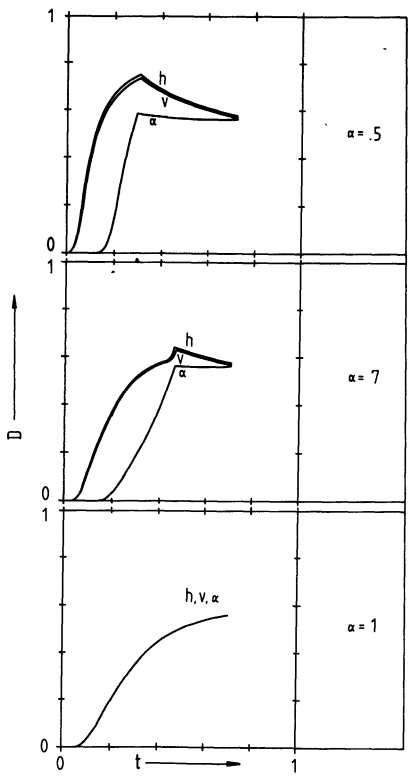

Fig. 7. — Density of domain walls *vs.* t for three different values of the modulation parameter.

6. Conclusions.

In this work, we have used a variational technique to deal with the problem of Ising phase transitions in frustrated 2D XY models. Our results (in good agreement with those obtained by numerical simulations [5, 7], earlier analytical approaches [8] and recent experimental work [9]) shows that the Ising character associated with the discrete symmetry is present all over the range of modulation above $\alpha = \frac{1}{3}$; it causes a double phase transition for $\alpha \neq 1$ and renormalize the critical temperature at $\alpha = 1$. For values of α in the interval $\left[\frac{1}{3}, 1\right]$ the picture that emerges is, as proposed in reference [7], those of an array of dipoles flipping around the center of α-bonds that undergoes an Ising transition at low temperatures. At a higher temperature, unbinding of thermal induced vortex-antivortex pairs (integer charges), causes a BKT transition. At $\alpha = 1$, there are no more fixed dipoles, and isotropic domains, by liberating fractional charges when growing, precipitates the BKT transition. The fact that the screening of Coulomb interaction is due to fractional charges does not seem to affect the value of the jump in helicity modulus at $\alpha = 1$. On another hand, the observed singularity of the specific heat [5] shows that the Ising character of the transition is always present in the isotropic case.

Topological order is observed to coexist with Ising disorder but not the contrary. We believe that this last property is a particularity of the model and not an universal feature [16]. In other words, we can imagine 2D systems in which the coupling between the Ising and the BKT variables allows topological disorder in the interior of Ising ordered domains. However in our system, the Ising order parameter in a sort of chirality measure of topological excitations and looses its sense when topological quasi-long-range order disappears.

The variational technique used in this paper is able to account not only for the double transition but also for the microscopic picture of the transition mechanism. In view of the preceding remark, we can trust our phase diagram of figure [7] and conclude that fractional charges remain confined at the Ising point for α approaching unity. Both transitions are always splitted and they merge only for $\alpha = 1$. This fact, proposed by H. Eikmans *et al.* [7] based on domain wall energy considerations, was, up to now, never contradicted by any experiment or numerical simulation.

Acknowledgments.

We would like to thank one of the referee of this paper for his clear and constructive suggestions.

This work has been supported by the Swiss National Science Foundation.

Appendix

Calculation of $\langle (\phi_i - \phi_j)^2 \rangle_{TR}$.

In order to use the density matrix ρ_{TR} of equation (3.3) to evaluate statistical averages, we shall first diagonalize the quadratic form H_{TR} :

$$H_{TR} = \sum_{\langle r, r' \rangle} \frac{1}{2} K_{rr'} (\phi(\mathbf{r}) - \phi(\mathbf{r}'))^2 . \tag{A1}$$

A four site basis is introduced on the array, in the following way :

$$\mathbf{r} = \mathbf{r}_{st}(\boldsymbol{\rho}) = \boldsymbol{\rho} + \frac{a}{2}(s\hat{\mathbf{x}} + t\hat{\mathbf{y}}) = \boldsymbol{\rho} + \mathbf{b}_{st} \tag{A2}$$

where

$$\boldsymbol{\rho} = 2a(n_x \hat{\mathbf{x}} + n_y \hat{\mathbf{y}}) \qquad \text{and} \qquad s = \pm 1 ; \qquad t = \pm 1$$

a being the lattice constant of the array, $\hat{\mathbf{x}}$ and $\hat{\mathbf{y}}$ the unit vectors on the x and y axes, n_x and n_y the integer coordinates of the center of the unit cell in the new array (see Fig. 8).

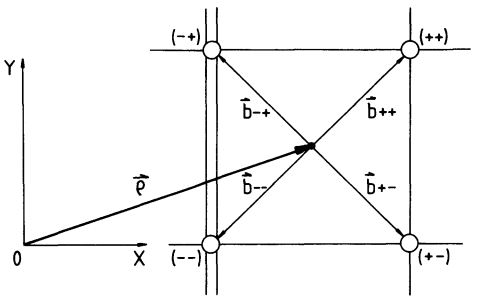

Fig. 8. — Parametrization of the lattice with basis introduced in equations (A2).

Expanding all functions of $\boldsymbol{\rho}$ in Fourier series, H_{TR} can be rewritten as follows :

$$H_{\mathrm{TR}} = \sum_{\mathbf{q}} \sum_{st} \sum_{s't'} \phi_{st}(\mathbf{q})\, M_{sts't'}(\mathbf{q})\, \phi^{*}_{s't'}(\mathbf{q}) \tag{A3}$$

the dynamical matrix $M(\mathbf{q})$ being given by :

$$\begin{pmatrix} (K_{\mathrm{v}} + K_{\mathrm{h}}) & -K_{\mathrm{v}} \cos(q_y) & -K_{\mathrm{h}} \cos(q_x) & 0 \\ -K_{\mathrm{v}} \cos(q_y) & (K_{\mathrm{v}} + K_{\mathrm{h}}) & 0 & -K_{\mathrm{h}} \cos(q_x) \\ -K_{\mathrm{h}} \cos(q_x) & 0 & (K_{\alpha} + K_{\mathrm{h}}) & -K_{\alpha} \cos(q_y) \\ 0 & -K_{\mathrm{h}} \cos(q_x) & -K_{\alpha} \cos(q_y) & (K_{\alpha} + K_{\mathrm{h}}) \end{pmatrix}. \tag{A4}$$

Its eigenvalues and eigenvectors are listed in the following table :

Eigenvalues :

$$\lambda_1 = K_{\mathrm{h}}\left[G\left(\frac{1-\cos q_y}{2}\right) + 1 - \sqrt{F^2\left(\frac{1-\cos q_y}{2}\right)^2 + \cos^2 q_x}\right]$$

$$\lambda_2 = K_{\mathrm{h}}\left[G\left(\frac{1-\cos q_y}{2}\right) + 1 + \sqrt{F^2\left(\frac{1-\cos q_y}{2}\right)^2 + \cos^2 q_x}\right]$$

$$\lambda_3 = K_{\mathrm{h}}\left[G\left(\frac{1+\cos q_y}{2}\right) + 1 - \sqrt{F^2\left(\frac{1+\cos q_y}{2}\right)^2 + \cos^2 q_x}\right]$$

$$\lambda_4 = K_{\mathrm{h}}\left[G\left(\frac{1+\cos q_y}{2}\right) + 1 + \sqrt{F^2\left(\frac{1+\cos q_y}{2}\right)^2 + \cos^2 q_x}\right].$$

Eigenvectors :

$$\mathbf{v}_1 = N_1[+1\,;+1\,;+r_1\,;+r_1]$$

$$\mathbf{v}_2 = N_2[+1\,;+1\,;+r_2\,;+r_2]$$

$$\mathbf{v}_3 = N_3[+1\,;-1\,;+r_3\,;-r_3]$$

$$\mathbf{v}_4 = N_4[+1\,;-1\,;+r_4\,;-r_4]$$

with the notations :

$$r^1_{(2)} = F\left(\frac{1-\cos q_y}{2\cos q_x}\right) \pm \sqrt{F^2\left(\frac{1-\cos q_y}{2\cos q_x}\right)^2 + 1}$$

$$r^3_{(4)} = F\left(\frac{1+\cos q_y}{2\cos q_x}\right) \pm \sqrt{F^2\left(\frac{1+\cos q_y}{2\cos q_x}\right)^2 + 1}$$

$$N_\sigma^2 = \frac{1}{2(1+r_\sigma^2)}\,; \qquad \sigma = 1, 2, 3, 4$$

$$F = \frac{K_\mathrm{v} - K_\alpha}{K_\mathrm{h}} \qquad \text{and} \qquad G = \frac{K_\mathrm{v} + K_\alpha}{K_\mathrm{h}}\,.$$

Thus, for each site $(\boldsymbol{\rho}\,; s\,; t)$ we can write :

$$\phi_{st}(\boldsymbol{\rho}) = \frac{1}{\sqrt{N}} \sum_{\mathbf{q}} \exp\left(i\,\frac{\mathbf{q}\cdot\boldsymbol{\rho}}{a} + i\,\frac{s}{2}\,q_x + i\,\frac{t}{2}\,q_y\right) \sum_\sigma a_\sigma(\mathbf{q}\,; s\,; t)\,\phi_\sigma(\mathbf{q}) \tag{A5}$$

where $a_\sigma(\mathbf{q}\,; s\,; t)$ is the (s, t) component of the eigenvector $\mathbf{v}_\sigma$ defined above. H_{TR} can then be expressed as follows :

$$H_{\mathrm{TR}} = \sum_{\mathbf{q}} \sum_{\sigma = 1,2,3,4} \lambda_\sigma(\mathbf{q})\,|\phi_\sigma(\mathbf{q})|^2 \tag{A6}$$

and the thermal averages $\langle|\phi_\sigma(\mathbf{q})|^2\rangle_{\mathrm{TR}}$ with the Gaussian density matrix (3.3) take the value :

$$\langle|\phi_\sigma(\mathbf{q})|^2\rangle_{\mathrm{TR}} = \frac{k_\mathrm{B}\,T}{2\,\lambda_\sigma(\mathbf{q})}\,.$$

We have now all the tools we need to perform the averages X_{ij} entering in equations (3.10) and (3.11).

As an example, we will compute X_h :

$$\begin{aligned} X_\mathrm{h} &= \langle(\phi_{-+}(\boldsymbol{\rho}) - \phi_{++}(\boldsymbol{\rho}))^2\rangle_{\mathrm{TR}} \\ &= \langle\phi^2_{-+}(\boldsymbol{\rho})\rangle_{\mathrm{TR}} + \langle\phi^2_{++}(\boldsymbol{\rho})\rangle_{\mathrm{TR}} - 2\langle\phi_{-+}(\boldsymbol{\rho})\,\phi_{++}(\boldsymbol{\rho})\rangle_{\mathrm{TR}} \\ &= \frac{1}{N}\sum_{\mathbf{q}}\sum_\sigma N_\sigma^2(1 + r_\sigma^2 - 2\,r_\sigma\cos q_x)\,\frac{k_\mathrm{B}\,T}{2\,\lambda_\sigma(\mathbf{q})}\,. \end{aligned} \tag{A7}$$

Approximating the q-dependent quantities by their small q limit, and replacing the sum $\sum_{\mathbf{q}}$ by an integral $\int \mathrm{d}^2q$ on a circular Brillouin zone of area π^2 we find :

$$X_{\mathrm{h}} \simeq \frac{k_{\mathrm{B}} T}{4 K_{\mathrm{h}}} \left\{ \frac{1}{1 + \sqrt{G/2}} + \frac{G(G+4) - F^2}{G(G+2) - F^2} \right\} .$$

In a similar way one finds :

$$\begin{aligned} X_{\mathrm{v}} &\simeq \frac{k_{\mathrm{B}} T}{4 K_{\mathrm{h}}} \left\{ \frac{1}{(1 + \sqrt{G/2})\sqrt{G/2}} + \frac{4(G+1-F)}{G(G+2) - F^2} \right\} \\ X_{\alpha} &\simeq \frac{k_{\mathrm{B}} T}{4 K_{\mathrm{h}}} \left\{ \frac{1}{(1 + \sqrt{G/2})\sqrt{G/2}} + \frac{4(G+1+F)}{G(G+2) - F^2} \right\} . \end{aligned} \tag{A8}$$

Expressions (A8) can be used directly in the iterative procedures of section 4.

However, a problem arises with the procedures when we reach T_{IS} from below : the X's diverge because the denominator $D = G(G+2) - F^2$ in equations (A8) goes to 0 at the transition. Indeed, at T_{IS} the Ising like order parameter S is 0. Thus, from equations (3.10) we get $4\alpha^2 ab - (a-\alpha)^2 = 0$, $G = (ab)^{1/2} - \alpha (b/a)^{1/2}$ and $F = (ab)^{1/2} + \alpha (b/a)^{1/2}$. Simple algebraic manipulations yields $G(G+2) - F^2 = 0$, or in an other form : $(G+1) = \sqrt{F^2+1}$.

This divergence is related to the softening of the third optical mode at the Ising transition, since for $q \to 0$ one can write :

$$\lambda_3(\mathbf{q}) \simeq K_{\mathrm{h}} \left\{ G + 1 - \sqrt{F^2+1} + \frac{1}{4\sqrt{F^2+1}} q_x^2 + \frac{F^2 - G\sqrt{F^2+1}}{4\sqrt{F^2+1}} q_y^2 \right\} \equiv \mu + O(q^2)$$

where $\mu \to 0$ at T_{IS}.

The softening of an optical mode is an usual signature of Ising transition in SCHA, and causes divergencies in two dimensions, since the dispersion relation goes as q^2.

However, we known from RG analysis [12] that the q dependence for 2D Ising models near the critical point is actually $q^{(2-1/4)}$. In order to avoid the difficulty we have chosen to replace the third eigenvalue in the small q approximation and near T_{IS} as follows :

$$\lambda_3 \simeq \Delta\mu + O(q^2) \tag{A9}$$

since this correction to the mass of the third optical mode will induce a correction of the denominator D near T_{IS} :

$$D = \Delta D \neq 0 . \tag{A10}$$

The above replacement is conceived in order to suppress the divergence at its origin. Quantitatively $\Delta\mu$ is chosen in order to simulate the effect of the actual power of q in the dispersion relation, when computing statistical averages :

$$\int_{\mathrm{BZ}} \mathrm{d}^2q \, \frac{1}{q^{7/4}} = \int_{\mathrm{BZ}} \mathrm{d}^2q \, \frac{1}{\Delta\mu + q^2} \tag{A11}$$

thus

$$\Delta\mu = \frac{\pi}{\exp\left(\dfrac{8}{\pi^{7/4}}\right) - 1} \sim 1.057 .$$

The actual dispersion relation of the third optical mode near the Ising critical point should be of the form :

$$\lambda_3 \simeq A q_x^{(2-1/4)} + B q_y^{(2-1/4)} .$$

It will be changed in :

$$\lambda^3 \simeq \Delta\mu\,(A + B) + A q_x^2 + B q_y^2$$

i.e., $[G + 1 - \sqrt{F^2 + 1}]$ will be changed in $\left[G + 1 + \frac{\Delta\mu\,(A + B)}{K_h} - \sqrt{F^2 + 1}\right]$.

Since we are interested in using the correction ΔD just close to the critical point, we can assume the relation $G + 1 = \sqrt{F^2 + 1}$ in evaluating it. Finaly, the expression of D (that comes from the product $\mu_3 \mu_4$) will be given, near T_{IS} by :

$$D = \Delta D = \frac{\Delta\mu}{2} \sqrt{F^2 + 1} \neq 0 \qquad \text{(A12)}$$

as we wish in expression (A9).

References

[1] For a recent review see : « Coherence in Superconducting networks », Nato advanced research workshop, Delft (Dec. 1987) *Physica B* **152** (1988).

[2] See e.g. HALSEY T. C., *J. Phys. C* **18** (1985) 2437 ; *Phys. Rev. B* **31** (1985) 5728.

[3] MARTINOLI P., Ref. [1] p. 146.

[4] TEITEL S. and JAYAPRAKASH C., *Phys. Rev. B* **27** (1983) 598.

[5] BERGE B., DIEP H. T., GHAZALI A. and LALLEMAND P., *Phys. Rev. B* **34** (1986) 3177.

[6] VILLAIN J., *J. Phys. C* **10** (1977) 1717.

[7] EIKMANS H., VAN HIMBERGEN J. E., KNOPS H.J.F. and THIJSSEN J. M., *Phys. Rev. B* **39** (1989) 11759.

[8] ARIOSA D., VALLAT A., BECK H., *Helv. Phys. Acta* **61** (1988) 244.

[9] THÉRON R., RENTSCH R., GAVILANO J., LEEMAN Ch. and MARTINOLI P., oral communication to the Swiss Physical Society (Oct. 1988).

[10] FISHMAN R. S., *Phys. Rev. B* **38** (1988) 11996.

[11] ARIOSA D. and BECK H. (to be published).

[12] See e.g. FISHER M. E., *Rev. Mod. Phys.* **46** (1974) 597.

[13] POKROVSKY V. L. and UIMIN G. V., *Phys. Lett. A* **45** (1973) 467.

[14] SIMANEK E. and STEIN K., *Physica A* **129** (1984) 40-61

[15] JOSÉ J. V., KADANOFF L. P., KIRKPATRICK S., NELSON D. R., *Phys. Rev. B* **16** (1977) 1217.

[16] KORSHUNOV S. E., *J. Phys. C* **19** (1986) 4427.